European Journal of Pharmaceutical Sciences 163 (2021) 105859

Contents lists available at ScienceDirect

European Journal of Pharmaceutical Sciences

journal homepage: www.elsevier.com/locate/ejps

Comparative EPR spectroscopy analysis of amphotericin B and miltefosine interactions with Leishmania, erythrocyte and macrophage membranes

Lais Alonso [a], Sebastião Antônio Mendanha [a], Rodrigo Saar Gomes [b], Miriam Leandro Dorta [b], Antonio Alonso [a,*]

[a] Instituto de Física, Universidade Federal de Goiás, Goiânia, GO, Brazil
[b] Instituto de Patologia Tropical e Saúde Publica, Departamento de Imunologia e Patologia Geral, Universidade Federal de Goiás, Goiânia, GO, Brazil

ARTICLE INFO

Keywords:
amphotericin B
miltefosine
Leishmania
macrophages
electron paramagnetic resonance

ABSTRACT

Electron paramagnetic resonance (EPR) spectroscopy of spin labels was used to study the interactions of amphotericin B (AmB) with the plasma membrane of Leishmania (L.) amazonensis promastigotes, human erythrocytes and J774.A1 murine macrophages, in comparison with reported and novel data for miltefosine (MIL). One of the objectives of this work is to look for the relationships between the activities of these two drugs in the Leishmania parasite with their changes in the cell membrane. A spin-labeled stearic acid inserted into the cell membranes showed strong interactions with putative AmB/sterol complexes, characterized by reductions in molecular dynamics. The concentration of the drugs in the plasma membrane that reduced the cell population by 50%, and the membrane-water partition coefficient of the drugs, were assessed. These biophysical parameters enabled estimates of possible therapeutic concentrations of these two drugs in the interstitial fluids of the tissues to be made. AmB displayed higher affinity for the plasma membrane of L. amazonensis than for that of the macrophage and erythrocyte, denoting a preference for a membrane that contains ergosterol. AmB also demonstrated higher hemolytic potential than MIL for measurements on erythrocytes in both PBS and whole blood. For MIL, the EPR technique detected membrane changes induced by the drug in the same concentration range that inhibited the growth of parasites, but in the case of AmB, an 8-fold higher concentration of the IC_{50} was necessary to observe a reduction in membrane fluidity, suggesting a better localized effect of AmB on the membrane. Taken together, the results demonstrate that the antiproliferative and cytotoxic effects of both drugs are associated with changes in cell membranes.

1. Introduction

Amphotericin B (AmB) is a polyene antibiotic produced by Streptomyces nodosus, which is considered the gold standard treatment for systemic fungal infections [1,2], and is widely used in the treatment of visceral and mucocutaneous leishmaniasis [3-5]. Since the early 1960s, AmB mixed with deoxycholate in the conventional commercial preparation of Fungizone has been used clinically with minimal development of microbial resistance [2,6]. Liposomal AmB has also been used for the past two decades to treat a broad range of fungal infections [7]. In this formulation, AmB incorporated into the liposome bilayer is able to maintain its antifungal activity whilst its toxicity is significantly reduced [7].

The most accepted and studied mechanism of action for AmB is the ion-channel model. According to this model, AmB-sterol complexes form ion-permeable channels in eukaryotic cell membranes that lead to cell death [8,9]. However, the mechanisms of AmB entry into the membrane and its interactions with lipids and proteins are still unclear [10,11]. More recently, studies using various techniques have shown that AmB does not enter a phosphatidylcholine (PC)-sterol model membrane, and can, in fact, extract ergosterol from the yeast cell membrane [6]. These findings gave rise to the sterol sponge model [6,10,11]. According to this hypothesis, AmB molecules form extramembranous sponge-like aggregates attached to the cell surface, which can extract ergosterol from the membrane, and thus could kill the fungi [6].

The advent of the sterol sponge model has raised doubts regarding the likelihood of AmB entering the membrane. In addition, the possible mechanisms of entry of AmB into the cell membrane and its flip-flop movement between the two leaflets of the membrane are not known. In contrast to the sterol sponge model, based on the demonstration that

* Corresponding author.
E-mail address: alonso@ufg.br (A. Alonso).

https://doi.org/10.1016/j.ejps.2021.105859
Received 9 September 2020; Received in revised form 1 April 2021; Accepted 19 April 2021
Available online 21 April 2021

AmB does not penetrate lipid bilayers, the spin label EPR data from a previous work [12] showed that, in fact, AmB does not enter model membranes but strongly suggested that it does readily enter a cell membrane, opening up new perspectives on the involvement of membrane proteins in the mechanism of action for AmB.

Miltefosine (MIL) is a synthetic phospholipid analogue (hexadecylphosphocholine), which is the preferred first-line drug for treatment of post-kala-azar dermal leishmaniasis (PKDL) in the Indian subcontinent [13]. MIL has demonstrated activity against several other Leishmania species [14,15], Trypanosoma cruzi [16], a broad spectrum of pathogenic fungi [17,18], various strains of Acanthamoeba [19], Streptococcus pneumoniae [20], various types of tumor cells [21] and Schistosoma mansoni [22]. However, MIL is an oral drug that has side effects related to its zwitterionic surfactant properties, these include gastrointestinal discomfort [23,24], anorexia, nausea, vomiting and diarrhoea [25]. Although the mechanisms of action for MIL are not yet well established, our research group has used EPR spectroscopy associated with the spin label method to show that MIL causes strong increases in the dynamics of L. amazonensis plasma membrane proteins for drug concentrations within the range of its leishmanicidal activity [26-29]. A mechanism based on the attack on the cell membrane is consistent with the reported broad spectrum of MIL activity against fungi, bacteria and protozoa.

Both AmB and MIL are amphiphilic and zwitterionic drugs that strongly interact with blood plasma albumin [7,30]. Based on the membrane-water and membrane-plasma partition coefficients, it has been estimated that the MIL concentration in the erythrocyte membrane is ~47,800 times higher than in water, but when considering whole blood, it is only ~59 times higher in the membrane than in blood plasma [31]. It is expected that in tissues where the concentration of albumin in the intersticial fluid is greatly decreased, the amount of MIL in the cell membranes should be much higher. Clinical pharmacokinetic data indicated that in visceral leishmaniasis patients, the MIL plasma concentration peaked at ~90 μg/mL [14]. On the other hand, a pharmacokinetic study in 27 lung transplant patients, who received nebulized liposomal AmB at a dose of 25 mg 3 times per week, found a mean AmB concentration of 11.1 mg/L after 2 days in the bronchioalveoar lavage fluid [32,7]. As AmB and MIL are active membrane drugs, it is interesting to know the proper concentration of each of them in the cell membrane to cause the death of a parasite and, from these data, make inferences about the possible concentrations in the cell medium.

Based on the antiproliferative and cytotoxic activities of a hydrophobic drug, our research group has developed a method to assess the membrane-water partition coefficient ($K_{M/W}$) of the drug, as well as its concentrations in the aqueous medium (c_{w50}) and in the plasma membrane (c_{m50}), which reduce the cell population by 50% [27,28,30,31,33-35]. In order to gain new insights into the mechanisms of action of AmB and MIL, a comparative study of these biophysical parameters was conducted for the two drugs in three types of cells: L. amazonensis promastigotes, human erythrocytes and J774.A1 murine macrophages. By measuring the minimal concentrations of AmB and MIL that cause changes in the cell membrane, as detected by EPR spectroscopy, an association between membrane alterations and antiproliferative/cytotoxic activities for these two drugs could be observed, suggesting that their primary action is on the cell membrane.

2. Materials and Methods

2.1. Chemicals

Grace's insect medium, RPMI-1640 medium, L-glutamine, penicillin G, streptomycin, hygromycin B, 3-(4,5-dimethylthiazol-2-yl)-2,5-diphenyl tetrazolium bromide (MTT), sodium bicarbonate, 5-doxyl-stearic acid (5-DSA) and AmB (A9528, colloidal suspension containing ~45% AmB, 35% sodium deoxycholate, sodium phosphate and sodium chloride) were purchased from Sigma-Aldrich (St. Louis, MO, USA). MIL was purchased from Avanti Polar Lipids Inc. (Alabaster, AL, USA). Heat-inactivated fetal bovine serum (FCS) was purchased from Corning Life Sciences (NY, USA).

2.2. Parasite and macrophage cells

Promastigotes of Leishmania (Leishmania) amazonensis (MHOM/BR/75/Josefa) reference strain and green fluorescent protein (GFP)-labeled L. amazonensis (IFLA/BR/67/PH8) were axenically cultured in 24-well microtiter plates containing 2 mL of Grace's insect medium supplemented with 20% FCS, 2 mM L-glutamine, 100 U/mL penicillin G and 100 μg/mL streptomycin, at 26°C, in anaerobic conditions as previously described [26-28]. The tests were performed with the parasites in the stationary phase of growth (6^{th} day of growth), according to previously published data [36]. The J774.A1 murine macrophage cell line was acquired from the cell bank of Rio de Janeiro (NCE/UFRJ). Cells were maintained in RPMI 1640 medium supplemented with 10% FCS, 2 mM L-glutamine, 100 U/mL penicillin G and 100 μg/mL streptomycin at 36.5°C in a humidified atmosphere (~95% RH) with 5% CO_2.

2.3. In vitro assays of antiproliferative and cytotoxic activity

Promastigotes of L. amazonensis or J774.A1 macrophages at several cell concentrations (5×10^6, 1×10^7, 1×10^8 and 5×10^8 parasites/mL; 5×10^5, 1×10^6, 4×10^6 and 1×10^7 macrophages/mL) were treated with increasing concentrations of AmB (0.01-100 μM) or MIL (1-2000 μM) in culture medium supplemented with 10% FCS in 96-well culture plates, using a total volume of 100 μL for parasites and 200 μL for macrophages. After a 24-h incubation period at 26°C for promastigotes and 36.5°C for macrophages, the cell viability was assessed based on the conversion of the water-soluble MTT to an insoluble formazan precipitate by viable mitochondria, which was allowed to develop for 2-5 h in the dark, according to previously published works [37,38]. MTT is a colorimetric assay for assessing cell metabolic activity, whereby the active NAD(P)H-dependent cellular oxidoreductase enzymes can give an indication of the number of viable cells. AmB or MIL, alone in the culture medium, does not generate detectable color. The percentage of viable cells relative to the untreated sample (control) was calculated for each compound concentration and the half-maximal inhibitory concentration (IC_{50}) or half-maximal cytotoxic concentration (CC_{50}) values of AmB and MIL were then determined by adjusting the concentration response data to a sigmoid curve [39].

2.4. Hemolytic potential of AmB and MIL

The blood was obtained from a university blood bank with a protocol approved by the Ethics Committee for Human and Animal Medical Research at Hospital das Clínicas, Universidade Federal de Goiás (CAAE: 81316417.1.0000.5078). After EDTA treatment, the blood was diluted three times in PBS and centrifuged at 800 x g for 10 min at 4°C. The plasma and white blood cells were removed by aspiration, and the pellet was resuspended in PBS. This washing procedure was repeated three times. Hemolytic tests with AmB and MIL were performed for five concentrations of erythrocytes: 1.11, 5.55, 11.11, 22.22 and 55.55×10^8 cells/mL. To calculate the cell concentration in the suspension, a volume of 90 fL was considered for the erythrocyte. AmB (containing ~45% AmB and ~35% sodium deoxycholate) was initially diluted at 10 mg/mL in PBS, and MIL was diluted at 20 mg/mL in ethanol; further dilutions were performed in PBS. After the treatment and incubation for 2 h at 36.5 ± 1°C, the volume of each sample was completed to 1.4 mL with PBS, and the samples were centrifuged again. The percentage of hemolysis was determined based on the absorbance of hemoglobin in the supernatant at 540 nm. The AmB or MIL concentration that caused 50% hemolysis (HC_{50}) was then determined by fitting the concentration response to a sigmoid curve.

To assess hemolytic potential in whole blood, the plasma was first

separated from cells by centrifugation at 2000 x g for 10 min at 4°C, and 58 μL plasma samples containing different AmB or MIL concentrations were prepared. Then 42 μl of the separated blood cells were added to each sample to reconstitute whole blood. The samples were gently stirred and incubated for 24 h at 7 ± 1°C. Hemolysis percentages were determined as described above.

2.5. Membrane spin labeling and treatment of the cells

For plasma membrane spin labeling, a film of the spin-labeled stearic acid (5-DSA) was first prepared at the bottom of a glass tube using a 1 μL aliquot of the spin probe dissolved in ethanol (2 mg/mL). After solvent evaporation, 1×10^8 cells suspended in 50 μL of FCS-free culture medium or PBS were added on the film of spin labels and the test tube was gently agitated. For treatment, the spin-labeled cells were diluted in order to obtain a specific concentration of cells/mL in medium containing AmB or MIL at an appropriate concentration and then the samples were agitated and incubated for 2 h at 36.5°C. After centrifugation at 20000 x g for 15 min, the volume of the spin-labeled, treated cells was adjusted to 50 μL again to be transferred to a 1-mm-i.d. capillary tube, which was flame-sealed, in order to perform the EPR measurements. The EPR spectra were recorded using an EMX-Plus spectrometer from Bruker (Rheinstetten, Germany), operating in the following instrumental settings: microwave power, 20 mW; microwave frequency, 9.452 GHz; modulation frequency, 100 kHz; modulation amplitude, 1.0 G; magnetic field scan, 100 G; sweep time, 168 s; and sample temperature, 25°C.

2.6. Data processing

The means and standard deviations were obtained from at least three independent experiments.

3. Results

3.1. Lipid dynamics in Leishmania, erythrocyte and macrophage membranes

The EPR spectra of the lipid spin label 5-DSA inserted in the plasma membrane of L. amazonensis promastigotes, erythrocytes and J774.A1 macrophages demonstrated remarkable reductions in dynamics after treatment of the cells with AmB. With addition of increasing AmB concentrations, the EPR parameter $2A_{//}$ (outer hyperfine splitting), associated with probe mobility, ranged from 55.5 to 59.5 G for L. amazonensis. A minimum AmB concentration required to observe an increase in $2A_{//}$ of at least 0.5 G (the experimental error) was estimated to be of 1×10^8 AmBs/cell, and to observe an increase of 3 G in $2A_{//}$ the required AmB concentration was approximately 4 times greater. To examine how this parameter is related to the effects of AmB on cell growth inhibition and cytotoxicity, we first sought to determine the drug concentration that causes an increase of 3 G in $2A_{//}$ for different cell concentrations used in the assay. Fig. 1A shows the EPR spectra of the spin label 5-DSA incorporated in L. amazonensis for different parasite concentrations that were treated with AmB concentrations sufficient to cause increases of ~3 G in the EPR spectral parameter $2A_{//}$ ($\Delta 2A_{//} = \sim 3$ G). With an increase in parasite concentration from 1×10^7 to 8×10^8 cells/mL (80-fold), the drug concentration required to produce an increase of ~3 G in $2A_{//}$ increased from 9 to 512 μM (57-fold).

For the J774.A1 macrophage membrane, the EPR spectra of 5-DSA showed a $2A_{//}$ of 52.8 G (Fig. 1B), indicating that the macrophage has a much more fluid membrane than that of Leishmania ($2A_{//}$ of 55.6 G, Fig. 1A) and erythrocyte ($2A_{//}$ of 57.2 G, Fig. 1C). In addition, the J774.A1 murine macrophage membrane was more fluid than that reported for the mouse peritoneal macrophage ($2A_{//}$ of ~55.0) [27]. At a macrophage concentration of 6.7×10^5 cells/mL, a concentration of 60 μM AmB caused a very large increase of 4.6 G in $2A_{//}$, while for 2.5×10^7 cells/mL a similar increase was only observed when the concentration of AmB was increased to 820 μM. We estimate that at a low macrophage concentration (5×10^5 cells/mL), an AmB concentration of ~20 μM would be sufficient to detect a change in plasma membrane lipid dynamics.

Figs. 1C and 1D show EPR spectra of 5-DSA in erythrocytes treated with MIL and AmB. In previous work using this same spin label, it was demonstrated that MIL enhances the plasma membrane fluidity of L. amazonensis promastigotes [26-28] and a similar effect is seen here for MIL-treated erythrocytes. For both MIL and AmB, increases in the erythrocyte concentration of 53x and 160x led to increases of 48x and 28x in the respective drug concentrations required to produce variations in $2A_{//}$ of approximately 3 G.

3.2. IC_{50}, HC_{50} and CC_{50} of AmB and MIL are assay-cell concentration dependent

Fig. 2 shows the cell concentration dependence of the parameters IC_{50} and HC_{50} for AmB and MIL against L. amazonensis promastigotes (panel A) and erythrocytes (panel B). The minimum drug concentrations necessary to cause detectable changes in the parameter $2A_{//}$ of the probe 5-DSA are also shown for each cell concentration used in the experiment. The AmB molar ratio between the IC_{50} and the minimum drug concentration necessary to produce a membrane alteration detected by EPR, was approximately 1:8. Although EPR spectroscopy using spin label is a technique of high reproducibility and notable sensitivity to monitor lipid dynamics in the cell membrane, it is not sensitive enough to detect localized changes in the membrane. Since the technique uses spin probe with a probe:lipid molar ratio of less than 1:100, the probes become spaced apart in the membrane and thus membrane changes are detected by the EPR spectra only when a probe fraction of at least ~25% is affected. However, in the case of MIL effects on L. amazonensis promastigotes, the EPR spectroscopy detected changes in plasma membrane dynamics at drug concentrations slightly lower than their IC_{50} values (Fig. 2A). This indicates that the effects of MIL on the parasite membrane are not very well localized as in the case of AmB.

EPR data for the erythrocyte showed a correlation with the HC_{50} values for both MIL and AmB (Fig. 2B). The AmB concentration necessary to observe a membrane change by EPR was ~3.5-fold higher than the HC_{50}. Interestingly, the hemolytic potential of AmB relative to MIL was lower at low concentrations of cells, but at high concentrations this relationship was reversed. Fig. 3 shows, for AmB, a comparison between the curves of IC_{50} and HC_{50} versus cell concentration. The projection of the fit curves indicated a greater difference between the HC_{50} and IC_{50} values for low cell concentrations, with the HC_{50}/IC_{50} ratio ranging from ~7 to ~2 between the cell concentrations of 5.5×10^7 and 2×10^9 cells/mL. Fig. 4 shows a comparison between EPR and CC_{50} data for macrophages treated with AmB. In this case, changes in the membrane were detected by EPR for an AmB concentration approximately 5x greater than the CC_{50} values.

3.3. Best-fit parameters $K_{M/W}$, c_{m50} and c_{w50}

As already mentioned above, our research group developed a method to determine the cell membrane-water partition coefficient, $K_{M/W}$, for hydrophobic compounds in cell suspension, as well as the compound concentrations in the cell membrane, c_{m50}, and aqueous phase, c_{w50}, that reduce the cell viability by 50%. This method is based on the variation of IC_{50}, CC_{50} or HC_{50} with the cell concentration used in the assay. Hydrophobic molecules accumulate in the cell membrane at high concentrations, making the drug distribution in the suspension inhomogeneous. For very dilute samples, the amount of membrane in the suspension is negligible and the measured IC_{50}, CC_{50} or HC_{50} values are similar to the corresponding c_{w50} values; whereas for high cell concentrations, a substantial fraction of the drug goes to the membrane and the drug concentration in the aqueous phase is much lower than that of suspension. The equation that describes the variation of IC_{50} with the

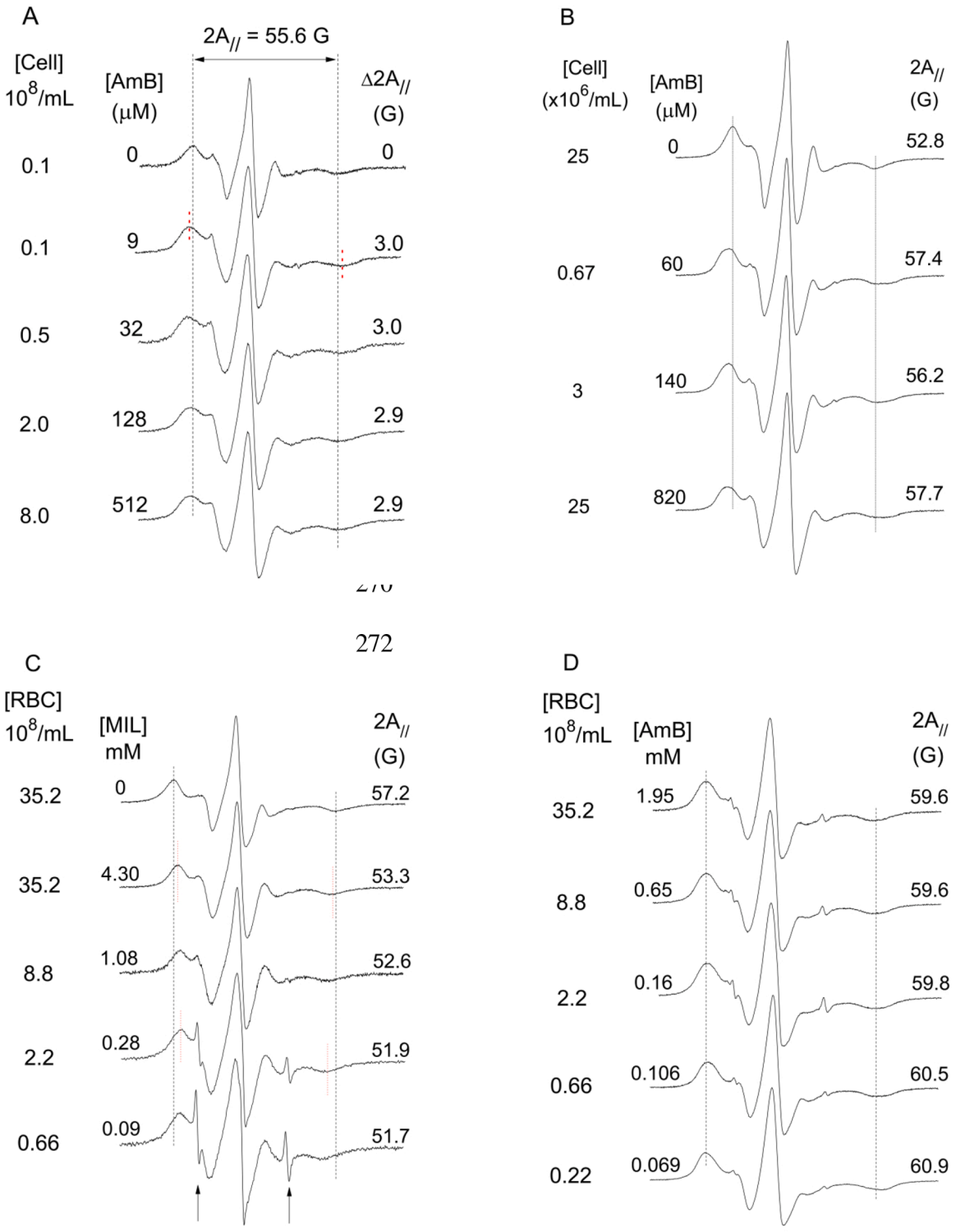

Fig. 1. EPR spectra of spin label 5-DSA in several plasma membrane: (A) Untreated (control) and AmB-treated Leishmania amazonensis promastigotes. The spectra shown are for samples of different parasite concentrations treated with AmB at a concentration sufficient to produce an increase of approximately 3 G in parameter $2A_{//}$ (external hyperfine splitting). The $2A_{//}$ is given by the magnetic-field separation between the first peak and the last inverted peak of the spectrum. (B) J774.A1 macrophage for samples with different cell concentrations and treated with AmB at concentrations necessary to increase the $2A_{//}$ parameter by 3.4 to 4.9 G. (C) and (D) Erythrocyte at different cell concentrations and treated with MIL (C) or AmB (D) at concentrations sufficient to cause large changes in the EPR parameter $2A_{//}$. The control EPR spectrum (for untreated erythrocytes) is the first in panel C. The arrows indicate unimportant resonance lines from a small fraction of spin label freely tumbling in the aqueous phase (outside the membrane), which is sometimes observed for samples with low cell concentration. In all EPR spectra the total scan range of the magnetic field was 100 G (X axis), and the intensity is in arbitrary units (Y axis).

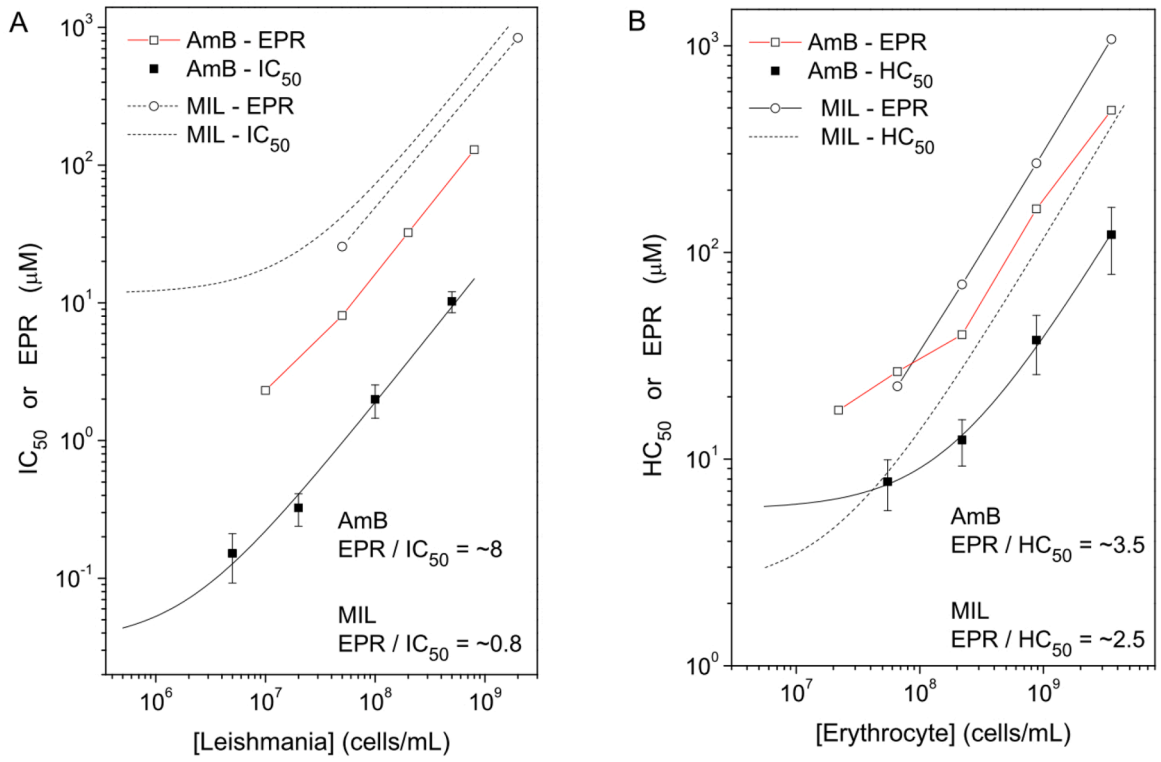

Fig. 2. (A) IC_{50} values of AmB and MIL for Leishmania amazonensis promastigotes at different initial cell concentrations. (B) HC_{50} values of AmB and MIL for several concentrations of erythrocyte in PBS. The EPR curves indicate concentrations of the compounds necessary to observe a change in the $2A_{//}$ of 5-DSA (~0.5 G). Data for MIL, represented by dashed curves, are from previous works and are shown for comparison in panels A [27] and B [30]. The best-fit curves shown are based on eq. 1 (presented below). The approximate molar ratios between the drug concentration to detect a membrane alteration by EPR and the IC_{50} or HC_{50} values are indicated for AmB and MIL.

cellular concentration was deduced in previous works [27,28], and is as follows:

$$IC_{50} = \left[\frac{(V_{mc} \cdot c_c)^{-1} + K_{M/W}}{(V_{mc} \cdot c_c)^{-1} + 1}\right] c_{w50}. \quad (1)$$

Where V_{mc} is the estimated membrane volume (in mL) for a single cell and c_c is the cell concentration per mL. Values of V_{mc} of 8.17×10^{-13} mL for a Leishmania amazonensis promastigote [27], 66.7×10^{-13} mL for a J774.A1 macrophage [33] and 10.5×10^{-13} mL for an erythrocyte [31] have previously been estimated. Unlike the values of IC_{50}, CC_{50} or HC_{50}, the parameters c_{w50} and c_{m50} do not depend on cell concentration.

From the fitting curves shown in Figs. 2 and 4, the best-fit parameters were obtained and are presented in Table 1. In comparison with MIL, AmB showed a higher affinity for the L. amazonensis promastigote membranes than for the macrophage and erythrocyte membranes, as deduced from the $K_{M/W}$ data, and it was also the molecule that required a lower concentration in the membrane to damage cells, as indicated by the c_{m50} data (Table 1). Interestingly, the fact that the c_{m50} value found for AmB was approximately 37 times smaller than that for MIL indicates that the attack of AmB on the membrane is better localized compared with MIL. Comparing the action of AmB on the Leishmania and erythrocyte membranes through the c_{w50} parameter, it is noted that the attack on the parasite is much greater than on the erythrocyte. This effect is largely explained by the fact that AmB has greater affinity for the promastigote membrane than that of the erythrocyte ($K_{M/W}$). This is a notable advantage for low cell concentrations, as can be seen in Fig. 3; while at high cellular concentrations, the ability of AmB to attack the Leishmania membrane rather than that of the erythrocyte is decreased. In addition, c_{m50} for AmB in the promastigote (20 mM) was only slightly lower than in the erythrocyte (32 mM) (Table 1).

3.4. Hemolytic potential in whole blood

Fig. 5 shows the hemolytic curves for AmB and MIL in whole blood. In this experiment, the drugs were diluted in the blood plasma separately and then the blood cells were added to the plasma to reconstitute the blood. AmB was much more hemolytic than MIL with a HC_{50} value approximately 7 times lower. As AmB obtained from Sigma was used in these experiments, which is a colloidal suspension containing ~45% AmB, 35% sodium deoxycholate, sodium phosphate and sodium chloride, the hemolytic potential of the surfactant deoxycholate was also measured. The HC_{50} value found for AmB was much lower than that of deoxycholate (4.94 mM). In PBS and at high cell concentrations, AmB and MIL had HC_{50} values of approximately 100 and 350 μM, respectively (Fig. 2B). However, in whole blood, HC_{50} values increased approximately 3x for AmB and 6x for MIL, suggesting that MIL has stronger interactions with blood plasma albumin. In previous work, using EPR spectroscopy, MIL has been shown to cause strong increases in the dynamics of plasma albumin [30].

4. Discussion

Membrane-water partition coefficient measurements indicated that AmB has much more affinity for the L. amazonensis membrane than for those of the erythrocyte and J774.A1 macrophage. For the erythrocyte and macrophage membranes, the $K_{M/W}$ values were respectively 119x and 21x lower than for L. amazonensis promastigotes (Table 1), demonstrating important selectivity for the parasite. Based on the values of HC_{50} (Fig. 5) and c_{m50} for the erythrocyte (Table 1), one can estimate the membrane-plasma partition coefficient for these drugs in whole blood, $K_{M/P}$, using an equation reported in a previous study [33]. The estimated $K_{M/P}$ values for MIL and AmB are 41 and 139, respectively, in contrast to the estimated $K_{M/W}$ values for red blood cells in PBS, of 48,

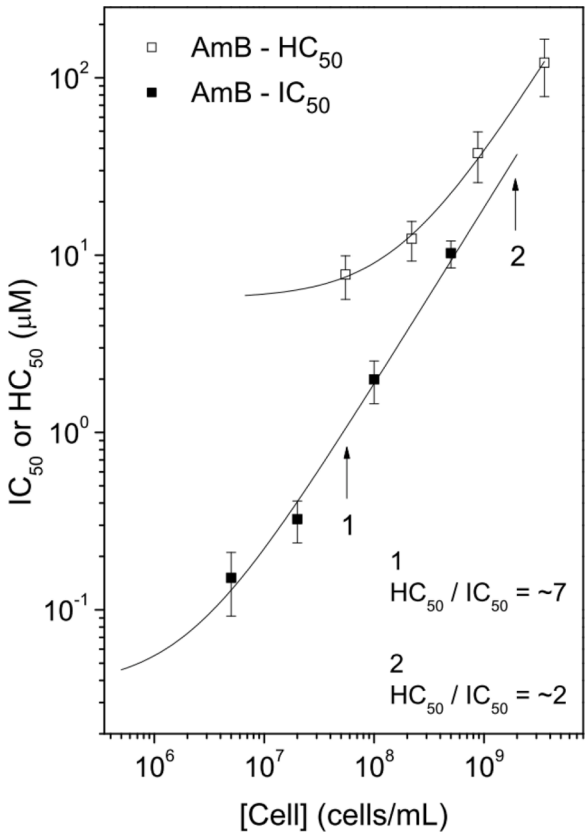

Fig. 3. Comparison between the AmB IC_{50} values for Leishmania amazonensis promastigotes and AmB HC_{50} values for erythrocytes in PBS at several cell concentrations (these data and best-fit curves have already been presented in Fig. 2). For the cell concentration of 5.5×10^7 cells/mL (indicated by an arrow in position 1) the estimated ratio of HC_{50} to IC_{50} was ~7 and for 2×10^9 cells/mL (position 2) this ratio dropped to ~2.

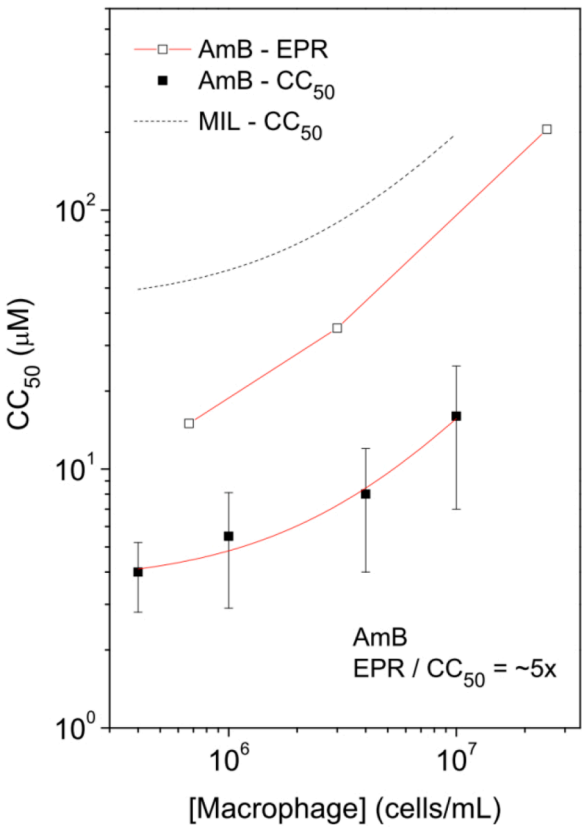

Fig. 4. CC_{50} values of AmB and MIL in J774.A1 murine macrophages for different initial cell concentrations. The approximate molar ratio between the drug concentration to detect a membrane alteration by EPR and the CC_{50} value are indicated. Data for MIL (dashed curve) are from a previous work [28].

000 and 5,600, respectively (Table 1). Both drugs have been shown to bind to plasma albumin [7,30] and these estimates indicate that albumin's ability to bind MIL instead of AmB is much greater. Our experimental data do not allow estimations of the $K_{M/P}$ of the drugs to be made for the case of Leishmania promastigotes in blood. However, from the $K_{M/W}$ values presented in Table 1, it is possible to infer that the partition coefficient for the parasite membrane would be much higher than for the erythrocyte. This means that in the bloodstream these drugs would be loaded more into the parasite's membranes than into those of the erythrocytes, and this does not depend on the number of parasites present in the blood. For the parasites located in tissues, where the albumin concentration in the interstitial fluid is very low, the partition coefficients of these drugs tend to their estimated $K_{M/W}$ values with cells in PBS, which are the very high values of 667,000 and 68,000 for AmB and MIL, respectively (Table 1). Thus, very low concentrations of these drugs in the interstitial fluid could lead to concentrations in the parasite's membrane high enough to kill it. Since the c_{m50} values were estimated at 20 mM for AmB and 734 mM for MIL (Table 1), these data allow us to estimate possible therapeutic concentrations against leishmaniasis in the tissue interstitial fluid as being only ~30 nM for AmB (20 mM/667,000) and ~11 μM for MIL (734 mM/68,000), which are the respective values found for c_{w50} (Table 1).

It is well known that AmB has a greater affinity for model and biological membranes containing ergosterol instead of cholesterol [6-11]. The results in Table 1 also show that the concentration of AmB in the membrane that inhibits cell growth by 50% (c_{m50} = 20 mM) is ~36x smaller than that of MIL (c_{m50} = 734 mM), indicating that the attack on the membrane exerted by AmB is much more located than in the case of MIL. This is in agreement with the pore-forming model, as the formation of few pores would be sufficient to impair the cell, in contrast to MIL which showed a more distributed action on the protein component of the membrane.

Table 1
Biophysical parameters $K_{M/W}$, c_{w50} and c_{m50} calculated from interactions of AmB and MIL with plasma membranes of L. amazonensis promastigotes, erythrocytes and J774.A1 macrophages.

Compound	$K_{M/W}$ (10^4)[a]	log $K_{M/W}$	c_{w50} (μM)	c_{m50} (mM)
Promastigotes				
AmB	66.7 ± 22.6	5.82	0.03 ± 0.01	20 ± 9
MIL[b]	6.8 ± 0.1	4.83	10.8 ± 3.0	734 ± 200
Erythrocytes (PBS)				
AmB	0.56 ± 0.13	3.75	5.7 ± 0.4	32 ± 3
MIL[c]	4.8	4.68	2.3	111
Macrophages				
AmB	3.2 ± 1.3	4.51	3.6 ± 1.7	115 ± 51
MIL[d]	5.35 ± 0.46	4.73	43.2 ± 2.2	2310 ± 230

[a] Best-fit parameters obtained by fitting the eq. 1 on the data from Figs. 2 and 4;[b,c,d]Data for MIL are from the references [27, 31] and [28], respectively.

Another experimental finding showed that the c_{m50} for the erythrocyte was approximately 1.5x greater than for the promastigote. This higher value found for the erythrocyte may be due to the short incubation period of these experiments (2 h at 36.5°C), since AmB-induced hemolysis has been reported to increase with the time of incubation [40]. Thus, although the partition coefficients for these two membranes are very different, the cytotoxic activities of AmB occurred at similar concentrations for these two cell types. Butler and co-authors [40] reported that when AmB at 6 mg/mL is added to a suspension of human erythrocytes, loss of potassium is the first event to be observed after 3

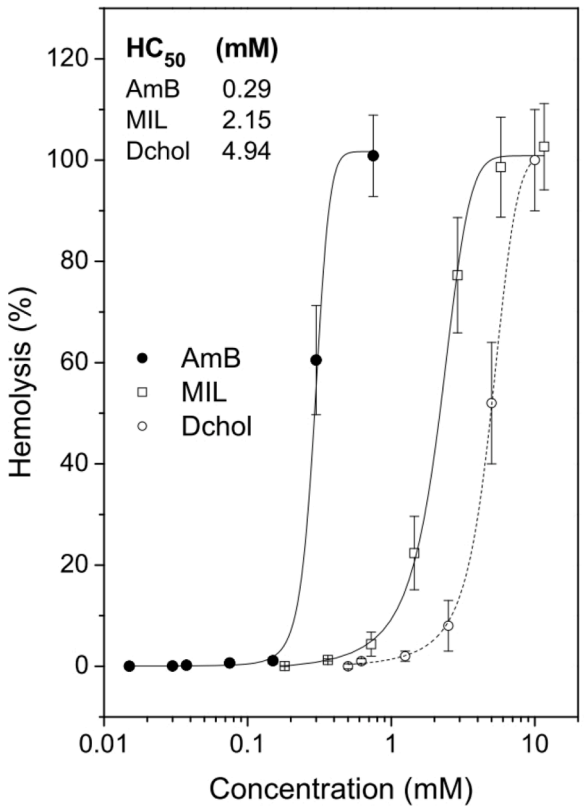

Fig. 5. Hemolytic curves for AmB, MIL and deoxycholate (Dchol) in whole blood after 24 h incubation at 7 ± 1°C. The HC_{50} values obtained from the fitting curves are indicated.

min, and as a result, sodium enters the cell. Furthermore, it has been shown that without AmB-induced Na^+ entry into erythrocytes, hemolysis does not occur [41]. The displacements of K^+ and Na^+ ions would lower the resting potential of the cell and increase the osmotic pressure, generating hemolysis.

It is worth mentioning that the hemolysis parameters shown in Table 1 are for measurements in PBS. For measurements in whole blood, the c_{m50} values of the two drugs should not change, however, the c_{w50} values found in PBS of 5.7 and 2.3 μM for AmB and MIL, respectively, may be much higher when PBS is replaced by plasma ($c_{plasma50}$). It has been reported that MIL binds to plasma albumin [30] and that AmB also has important interactions with blood plasma [42]. In fact, AmB and MIL HC_{50} values in whole blood were 0.29 and 2.15 mM, respectively (Fig. 5). It has also been shown that the hemolytic effect of MIL in whole blood increases with the incubation time at 5°C for a period of at least 24 h [31]. These results indicate that plasma albumin protects red blood cells (RBCs) from the hemolytic effects of the drug and that albumin may function as a MIL delivery system. Thus, therapeutic administration could perhaps be done intravenously after previous dilution of MIL in the patient's blood plasma separately.

The fact that AmB has greater affinity for the parasite plasma membrane compared to that of the erythrocyte leads to greater AmB activity against the parasite in assays with low cell concentrations, but for higher cell concentrations this advantage is greatly diminished (Fig. 3). Likewise, the fact that AmB has a greater affinity than MIL for the parasite membrane increases the difference in the activity of the two drugs for low cell concentrations. For example, at a concentration of 5×10^6 cells/mL the ratio between the IC_{50} values of MIL and AmB was ~100, but at a concentration of 5×10^8 cells/mL this ratio drops to ~33 (Fig. 2A). This effect occurs because the c_{w50} value is independent of the cell concentration. Thus, with the aqueous volume being smaller for suspensions with a high cell concentration, a smaller number of drug molecules remains in the water in micellar or aggregate form. This type of effect gains importance when considering that in the physiological condition cell concentrations are high, as in the case of blood, where there are approximately 5×10^9 RBCs/mL.

In general, EPR spectroscopy detected alterations in membrane promoted by AmB at lower concentrations than for MIL, suggesting that the hydrophobic surfaces of the AmB/sterol complexes interact strongly with the spin label, causing motional restriction of the probe. This work dealt with the dependence of the antiproliferative and cytotoxic activities of the drugs on the concentration of cells used in the experiments. For both drugs, measurements in assays with different cell concentrations showed a correlation between the concentrations required for alterations in membrane detected by EPR, and the respective IC_{50} values. This result suggests that the antiproliferative and cytotoxic activities of the drugs are associated with changes in the plasma membrane. Since the changes in the cell membrane are associated with hemolysis (Fig. 2B), or lysis of the parasites as demonstrated in a previous work [26], both drugs must cause electrolyte leakage in the cells. In fact, the EPR results suggest that the mechanism of action of MIL, like that of AmB, is an attack on the parasite plasma membrane and that other effects reported in the literature [14] may be consequences of the primary action of the drug on the membrane.

Experiments with macrophages infected with L. amazonensis have shown that AmB and MIL are capable of reducing infections in murine macrophages and that AmB has a significantly greater leishmanicidal action than MIL [43,44]. However, the mechanisms of AmB in particular for reaching amastigotes within a parasitophorous vacuole are not known. According to the sterol sponge model, AmB should be located as AmB/sterol aggregates on the outside of macrophages. Two membrane barriers need to be penetrated by AmB to gain access to the amastigotes. From the macrophage plasma membrane, it needs to reach the parasitophorous vacuole membrane, likely by passive diffusion, and then enter the parasite membrane via membrane transporters, endocytosis or diffusion [45].

5. Conclusions

Spin label EPR spectroscopy suggested strong plasma membrane rigidity upon AmB-treatment of Leishmania (L.) amazonensis promastigotes, erythrocytes and J774.A1 macrophages, probably caused by the interactions of the spin probe with the hydrophobic surfaces of AmB/sterol complexes. The concentration of AmB in the membrane that inhibited the growth of the parasite by 50% (c_{m50}) was approximately 36x less than that of MIL, indicating that the attack of AmB, compared with MIL, is more efficient and well localized in the membrane. The concentrations of AmB and MIL that caused changes in the membrane detected by EPR showed a correlation with the antiproliferative and cytotoxic activities of the drugs. In whole blood, the AmB concentration required for 50% hemolysis (HC_{50}) was approximately 7x less than that of MIL. Since it has been shown that AmB does not penetrate the lipid bilayer of phospholipid/sterol, but the EPR spectroscopy suggests its rapid entry into the plasma membrane, it would be interesting to know whether membrane proteins play a role in the mechanism of AmB penetration into the cell membrane.

CRediT authorship contribution statement

Lais Alonso: Conceptualization, Formal analysis, Investigation, Methodology, Project administration, Validation, Visualization, Writing - original draft. **Sebastião Antônio Mendanha:** Conceptualization, Formal analysis, Methodology, Visualization, Writing - original draft. **Rodrigo Saar Gomes:** Conceptualization, Formal analysis, Methodology, Writing - original draft. **Miriam Leandro Dorta:** Conceptualization, Formal analysis, Funding acquisition, Methodology, Writing - original draft. **Antonio Alonso:** Conceptualization, Formal analysis, Investigation, Methodology, Project administration, Validation,

Visualization, Writing - review & editing.

Declaration of Competing Interest

The authors declare no conflicts of interest.

Acknowledgements

This study was financially supported by grants from the Brazilian research funding agencies CNPq (445666/2014-5 and 406521/2016-6), CAPES and FAPEG (201210267001110). Lais Alonso was a recipient of a postdoctoral fellowship from CNPq (150369/2018-2) and is currently a postdoctoral fellow at CAPES. Antonio Alonso received a research grant from CNPq (304122/2019-0).

References

[1] Mouri, R, Konoki, K, Matsumori, N, Oishi, T, Murata, M, 2008. Complex formation of amphotericin B in sterol-containing membranes as evidenced by surface plasmon resonance. Biochemistry 47, 7807–7815. https://doi.org/10.1021/bi800334p.
[2] Cohen, B E, 2010. Amphotericin B membrane action: role for two types of ion channels in eliciting cell survival and lethal effects. J. Membrane Biol. 238, 1–20. https://doi.org/10.1007/s00232-010-9313-y.
[3] Berman, JD, 1997. Human leishmaniasis: clinical, diagnostic and chemotherapeutic developments in past 10 years. Clin. Infect. Dis. 24 684e70310.1093/clind/24.4.684.
[4] Kothandaraman, GP, Ravichandran, V, Bories, C, Loiseau, PM, Jayakrishnan, A, 2017. Anti-fungal and anti-leishmanial activities of pectin-amphotericin B conjugates. J. Drug Deliv. Sci. Technol. 39, 1–7. https://doi.org/10.1016/j.jddst.2017.02.010.
[5] Sundar, S, Agarwal, D, 2018. Visceral Leishmaniasis-Optimum Treatment Options in Children. Pediatr. Infect. Dis. J. 37 (5), 492–494. https://doi.org/10.1097/INF.0000000000001885.
[6] Anderson, TM, Clay, MC, Cioffi, AG, Diaz, KA, Hisao, GS, Tuttle, MD, Nieuwkoop, AJ, Comellas, G, Maryum, N, Wang, S, Uno, BE, Wildeman, EL, Gonen, T, Rienstra, CM, Burke, MD, 2014. Amphotericin forms an extramembranous and fungicidal sterol sponge. Nat. Chem. Biol. 10 (5), 400–406. https://doi.org/10.1038/nchembio.1496.
[7] Stone, NR, Bicanic, T, Salim, R, Hope, W, 2016. Liposomal Amphotericin B (AmBisome(®)): A review of the pharmacokinetics, pharmacodynamics, clinical experience and future directions. Drugs 76 (4), 485–500. https://doi.org/10.1007/s40265-016-0538-7.
[8] Kamiński, DM, 2014. Recent progress in the study of the interactions of amphotericin B with cholesterol and ergosterol in lipid environments. Eur. Biophys. J. 43, 453–467. https://doi.org/10.1007/s00249-014-0983-8.
[9] Kristanc, L, Božič, B, Jokhadar, ŠZ, Dolenc, MS, Gomišček, G, 2019. The pore-forming action of polyenes: From model membranes to living organisms. Biochim. Biophys. Acta Biomembr. 1861 (2), 418–430. https://doi.org/10.1016/j.bbamem.2018.11.006.
[10] Gray, KC, Palacios, DS, Dailey, I, Endo, MM, Uno, BE, Wilcock, BC, Burke, MD, 2012. Amphotericin primarily kills yeast by simply binding ergosterol. Proc. Natl. Acad. Sci. U S A 109 (7), 2234–2239. https://doi.org/10.1073/pnas.1117280109.
[11] Palacios, DS, Dailey, I, Siebert, DM, Wilcock, BC, Burke, MD, 2011. Synthesis-enabled functional group deletions reveal key underpinnings of amphotericin B ion channel and antifungal activities. Proc. Natl. Acad. Sci. U S A. 108 (17), 6733–6738. https://doi.org/10.1073/pnas.1015023108.
[12] Alonso, L, Mendanha, SA, Dorta, ML, Alonso, A, 2020. Analysis of the Interactions of Amphotericin B with the Leishmania Plasma Membrane Using EPR Spectroscopy. J. Phys. Chem. B. 124 (45), 10157–10165. https://doi.org/10.1021/acs.jpcb.0c07721.
[13] Ramesh, V, Dixit, KK, Sharma, N, Singh, R, Salotra, P, 2020. Assessing the Efficacy and Safety of Liposomal Amphotericin B and Miltefosine in Combination for Treatment of Post Kala-Azar Dermal Leishmaniasis. J. Infect. Dis. 221 (4), 608–617. https://doi.org/10.1093/infdis/jiz486.
[14] Dorlo, T.P, Balasegaram, M, Beijnen, JH, de Vries, PJ, 2012. Miltefosine: a review of its pharmacology and therapeutic efficacy in the treatment of leishmaniasis. J. Antimicrob. Chemother. 67, 2576–2597. https://doi.org/10.1093/jac/dks275.
[15] Morais-Teixeira, Ed, Damasceno, QS, Galuppo, MK, Romanha, AJ, Rabello, A, 2011. The in vitro leishmanicidal activity of hexadecylphosphocholine (miltefosine) against four medically relevant Leishmania species of Brazil. Mem. Inst. Oswaldo Cruz 106 (4), 475–478. https://doi.org/10.1590/s0074-02762011000400015.
[16] Croft, SL, Seifert, K, Duchêne, M, 2003. Antiprotozoal activities of phospholipid analogues. Mol. Biochem. Parasitol. 126, 165–172. https://doi.org/10.1016/S0166-6851(02)00283-9.
[17] Widmer, F, Wright, LC, Obando, D, Handke, R, Ganendren, R, Ellis, DH, Sorrell, TC, 2006. Hexadecylphosphocholine (miltefosine) has broad-spectrum fungicidal activity and is efficacious in a mouse model of cryptococcosis. Antimicrob. Agents Chemother. 50, 414–421. https://doi.org/10.1128/AAC.50.2.414-421.2006.
[18] Spadari, CC, de Bastiani, FWMDS, Lopes, LB, Ishida, K, 2019. Alginate nanoparticles as non-toxic delivery system for miltefosine in the treatment of candidiasis and cryptococcosis. Int. J. Nanomedicine 14, 5187–5199. https://doi.org/10.2147/IJN.S205350.
[19] Lorenzo-Morales, J, Khan, NA, Walochnik, J, 2015. An update on Acanthamoeba keratitis: diagnosis, pathogenesis and treatment. Parasite 22, 10. https://doi.org/10.1051/parasite/2015010.
[20] Llull, D, Rivas, L, García, E, 2007. In vitro bactericidal activity of the antiprotozoal drug miltefosine against Streptococcus pneumoniae and other pathogenic streptococci. Antimicrob. Agents Chemother. 51, 1844–1848. https://doi.org/10.1128/AAC.01428-06.
[21] Van Blitterswijk, WJ, Verheij, M, 2008. Anticancer alkylphospholipids: mechanisms of action, cellular sensitivity and resistance, and clinical prospects. Curr. Pharm. Des. 14, 2061–2074. https://doi.org/10.2174/138161208785294636.
[22] Eissa, MM, El-Moslemany, RM, Ramadan, AA, Amer, EI, El-Azzouni, MZ, El-Khordagui, LK, 2015. Miltefosine Lipid Nanocapsules for Single Dose Oral Treatment of Schistosomiasis Mansoni: A Preclinical Study. PLoS One 10 (11) e014178810.1371/journal.pone.0141788. eCollection 2015.
[23] Crul, M, Rosing, H, de Klerk, GJ, Dubbelman, R, Traiser, M, Reichert, S, Knebel, NG, Schellens, JH, Beijnen, JH, Bokkel, ten, Huinink, WW, 2002. Phase I and pharmacological study of daily oral administration of perifosine (D-21266) in patients with advanced solid tumours. Eur. J. Cancer 38 (12), 1615–1621. https://doi.org/10.1016/s0959-8049(02)00127-2.
[24] Petit, K, Suwalsky, M, Colina, JR, Aguilar, LF, Jemiola-Rzeminska, M, Strzalka, K, 2019. In vitro effects of the antitumor drug miltefosine on human erythrocytes and molecular models of its membrane. Biochim. Biophys. Acta Biomembr. 1861 (1), 17–25. https://doi.org/10.1016/j.bbamem.2018.10.009.
[25] World Health Organization. 2010. Control of the leishmaniasis: report of a meeting of the WHO Expert Committee on the Control of Leishmaniases, Geneva, 22-26 March 2010. (WHO technical report series; no. 949).
[26] Moreira, RA, Mendanha, SA, Fernandes, KS, Matos, GG, Alonso, L, Dorta, ML, Alonso, A, 2014. Miltefosine increases lipid and protein dynamics in Leishmania amazonensis membranes at concentrations similar to those needed for cytotoxicity activity. Antimicrob. Agents Chemother. 58, 3021–3028. https://doi.org/10.1128/AAC.01332-13.
[27] Fernandes, KS, de Souza, PE, Dorta, ML, Alonso, A, 2017. The cytotoxic activity of miltefosine against Leishmania and macrophages is associated with dynamic changes in plasma membrane proteins. Biochim. Biophys. Acta. 1859 (1), 1–9. https://doi.org/10.1016/j.bbamem.2016.10.008.
[28] Alonso, L, Cardoso, ÉJS, Gomes, RS, Mendanha, SA, Dorta, ML, Alonso, A, 2019. Antileishmanial and cytotoxic activities of ionic surfactants compared to those of miltefosine. Colloids Surf. B Biointerfaces 183, 110421. https://doi.org/10.1016/j.colsurfb.2019.110421.
[29] Scariot, DB, Britta, EA, Moreira, AL, Falzirolli, H, Silva, CC, Ueda-Nakamura, T, Dias-Filho, BP, Nakamura, CV, 2017. Induction of Early Autophagic Process on Leishmania amazonensis by Synergistic Effect of Miltefosine and Innovative Semi-synthetic Thiosemicarbazone. Front. Microbiol. 8, 255. https://doi.org/10.3389/fmicb.2017.00255.
[30] Alonso, L, Cardoso, EJS, Mendanha, SA, Alonso, A, 2019. Interactions of miltefosine with erythrocyte membrane proteins compared to those of ionic surfactants. Colloids Surf. B Biointerfaces 180, 23–30. https://doi.org/10.1016/j.colsurfb.2019.04.040.
[31] Alonso, L, Alonso, A, 2016. Hemolytic potential of miltefosine is dependent on cell concentration: implications for in vitro cell cytotoxicity assays and pharmacokinetic data. Biochim. Biophys. Acta 1858, 1160–1164. https://doi.org/10.1016/j.bbamem.2016.03.004.
[32] Monforte, V, Ussetti, P, López, R, Gavaldà, J, Bravo, C, de Pablo, A, Pou, L, Pahissa, A, Morell, F, Román, A, 2009. Nebulized liposomal amphotericin B prophylaxis for Aspergillus infection in lung transplantation: pharmacokinetics and safety. J. Heart Lung Transplant. 28 (2), 170–175. https://doi.org/10.1016/j.healun.2008.11.004.
[33] Alonso, L, Fernandes, KS, Mendanha, SA, Gonçalves, PJ, Gomes, RS, Dorta, ML, Alonso, A, 2019. In vitro antileishmanial and cytotoxic activities of nerolidol are associated with changes in plasma membrane dynamics. Biochim. Biophys. Acta 1861, 1049–1056. https://doi.org/10.1016/j.bbamem.2019.03.006.
[34] Alonso, L, Menegatti, R, Gomes, RS, Dorta, ML, Luzin, RM, Lião, LM, Alonso, A, 2020. Antileishmanial activity of the chalcone derivative LQFM064 associated with reduced fluidity in the parasite membrane as assessed by EPR spectroscopy. Eur. J. of Pharm. Sci. 151, 105407 https://doi.org/10.1016/j.ejps.2020.105407.
[35] Alonso, L, de Paula, JC, Baréa, P, Sarragiotto, MH, Nakamura, TU, Alonso, A, Fernandes, NS, Lancheros, CAC, Volpato, H, Bidóia, DL, Nakamura, CV, 2021. Membrane dynamics in Leishmania amazonensis and antileishmanial activities of β-carboline derivatives. Biochim. Biophys. Acta Biomembranes 1863, 183473. https://doi.org/10.1016/j.bbamem.2020.183473.
[36] da Silva Jr, IA, Morato, CI, Quixabeira, VB, Pereira, LI, Dorta, ML, de Oliveira, MA, Horta, MF, Ribeiro-Dias, F, 2015. In vitro metacyclogenesis of Leishmania (Viannia) braziliensis and Leishmania (Leishmania) amazonensis clinical field isolates, as evaluated by morphology, complement resistance, and infectivity to human macrophages. Biomed. Res. Int., 393049 https://doi.org/10.1155/2015/393049, 2015.
[37] Mosmann, T, 1983. Rapid colorimetric assay for cellular growth and survival: application to proliferation and cytotoxicity assays. Journal of Immunological Methods 65 (1–2), 55–63. https://doi.org/10.1016/0022-1759(83)90303-4.
[38] Cory, AH, Owen, TC, Barltrop, JA, Cory, JG, 1991. Use of an aqueous soluble tetrazolium/formazan assay for cell growth assays in culture. Cancer Communications 3 (7), 207–212. https://doi.org/10.3727/095535491820873191.

[39] Harris, L, Frick, P, Garbett, S, Hardeman, KN, Paudel, BB, Lopez, CF, Quaranta, V, Tyson, DR, 2016. An unbiased metric of antiproliferative drug effect in vitro. Nat. Methods 13, 497–500. https://doi.org/10.1038/nmeth.3852.

[40] Butler, WT, Alling, DW, Cotlove, E, 1965. Potassium los from human erythrocytes exposed to Amphotericin B. Proc. Soc. Exp. Biol. Med. 118, 297–300. https://doi.org/10.3181/00379727-118-29825.

[41] Szponarski, W, Bolard, J, 1987. Temperature-dependent modes for the binding of the polyene antibiotic amphotericin B to human erythrocyte membranes. A circular dichroism study. Biochim. Biophys. Acta 897 (2), 229–237.

[42] Stone, NR, Bicanic, T, Salim, R, Hope, W, 2016. Liposomal Amphotericin B (AmBisome(®)): A review of the pharmacokinetics, pharmacodynamics, clinical experience and future directions. Drugs 76 (4), 485–500. https://doi.org/10.1007/s40265-016-0538-7.

[43] Neal, RA, Croft, SL, 1984. An in-vitro system for determining the activity of compounds against the intracellular amastigote form of Leishmania donovani. J. Antimicrob. Chemother. 14 (5), 463–475. https://doi.org/10.1093/jac/14.5.463.

[44] Garcia, AR, Amaral, ACF, Azevedo, MMB, Corte-Real, S, Lopes, RC, Alviano, CS, Pinheiro, AS, Vermelho, AB, Rodrigues, IA, 2017. Cytotoxicity and anti-Leishmania amazonensis activity of Citrus sinensis leaf extracts. Pharm Biol 55 (1), 1780–1786. https://doi.org/10.1080/13880209.2017.1325380.

[45] Croft, SL, Coombs, GH, 2003. Leishmaniasis-current chemotherapy and recent advances in the search for novel drugs. Trends Parasitol 19 (11), 502–508. https://doi.org/10.1016/j.pt.2003.09.008.